XIX International Conference on Water Resources
CMWR 2012
University of Illinois at Urbana-Champaign
June 17-22, 2012

ADVECTION IN IN BIOIRRIGATED MUDDY SEDIMENTS-CAN IT BE RELEVANT? A MODEL STUDY

Andreas Brand[*,#,†], **Joerg Lewandowski**[†], **Enrico Hamann**[+] **and Gunnar Nuetzmann**[†]

[*] Eawag, Swiss Federal Institute of Aquatic Science and Technology,
Kastanienbaum, Switzerland
e-mail: andreas.brand@eawag.ch

[#] Institute of Biogeochemistry and pollutant dynamics
ETH Zurich, Switzerland

[†] Leibniz-Institute of Freshwater Ecology and Inland Fisheries
Mueggelseedamm 310, Berlin, Germany

+ Hydrogeology group,
Free University of Berlin,
Malteserstrasse74-100, Berlin, Germany

Key words: Solute transport, sediments, bioirrigation

1 INTRODUCTION

It is commonly accepted that tube dwelling macroinvertebrates play a significant role in the solute dynamics of marine and lacustrine sediments. The influence of these organisms ranges from mixing of the solid sediment phase by burrowing (bioturbation) to flushing of the sediment with surface water by pumping activity in the burrows (bioirrigation).

While bioturbation results in a transport of highly reactive, freshly sedimented organic material into deeper zones of the sediment, the consequences of bioirrigation are even more complex. The transport of oxygen containing surface water into the deeper zones of the sediment triggers a sequence of redox reactions, which can heavily influence the ecology of the whole lake system. For example, the inserted oxygen results in the formation of iron oxides in the close vicinity of the tube walls in iron-rich sediments. These oxides can bind phosphate and potentially leads to a long-term removal of this important nutrient which frequently limits the trophic state of lakes.

A typical bioirrigating macroinvertebrate is the non-biting midge lava *Chironomus plumosus*, which is frequently found in muddy freshwater sediments in high abundance (typical population density of 1,000 ind. m^{-2}, but densities of up to 100,000 ind. m^{-2} have been reported). This larva builds U-shaped up to 20 cm deep burrows of 1.5-2 mm diameter tubes. The burrows are flushed in regular intervals. *C. plumosus* larvae pump surface water through their tube with an average velocity of 1.5 cm s^{-1} and peak velocities of 3.5 cm s^{-1} were observed in the center of the tube

outlet[1]. In a laboratory study a typical pumping activity with a frequency of 26 h^{-1} and pumping intervals of 90 s was observed[2].

In an additional study, 18-F fluoride positron emission tomography was used to investigate the influence of the pumping activity on the spreading of an inert tracer in the sediment surrounding the burrow[3]. It was found that the growth of the tracer plume at the outlet branch of the burrow was faster than at the inlet branch of the burrow[3]. This result suggested that this difference in spreading of the tracer is due to advection in the sediment driven by the pressure gradient resulting from the pumping activity of the chironomid larva[3]. Until now, macroinvertebrate induced advection has only been reported for sandy coastal sediments inhabited by species like *Arenicola marina* which live in blindly ending L-shaped tubes and press water into the sediment at the end of the tube by peristaltic movements[4].

In this paper we assess the plausibility and potential impact of bioirrigation induced advective flow in sediments surrounding burrows as they are typical for organisms like *C. plumosus*. We used a simplified 2-D model of an idealized U-shaped burrow which couples the free fluid flow in the burrow with the porous media flow in the sediment.

2 MODEL SETUP

2.1 Governing equations

The model was implemented using the finite element code COMSOL (Version 4.1). The conceptual model and its dimensions is given in Figure 1a. The model area was subdivided into three parts with different flow regimes. The flow inside the tube was calculated using the Navier-Stokes equation for incompressible laminar flow,

$$\rho\left(\frac{\partial \mathbf{u}}{\partial t} + \mathbf{u}\cdot\nabla\mathbf{u}\right) = -\nabla p + \mu\nabla^2\mathbf{u}$$
$$\rho\nabla\cdot\mathbf{u} = 0 \tag{1}$$

where $\mathbf{u}$ denotes the velocity field, p the pressure, ρ the density of water (1000 kg m^{-3}) and μ the dynamic viscosity of water (0.001 Pa s).The fluid flow in the sediment was calculated using Darcy's law,

$$\rho\nabla\cdot\mathbf{u} = 0$$
$$\mathbf{u} = -\frac{\kappa}{\mu}\nabla p \tag{2}$$

where κ denotes the permeability of the porous medium. In the presented study, model runs were performed with κ ranging from 10^{-14} to 10^{-11} m^2. These values cover the range as they are typical for unconsolidated loamy fine sediments to sandy sediments[5].

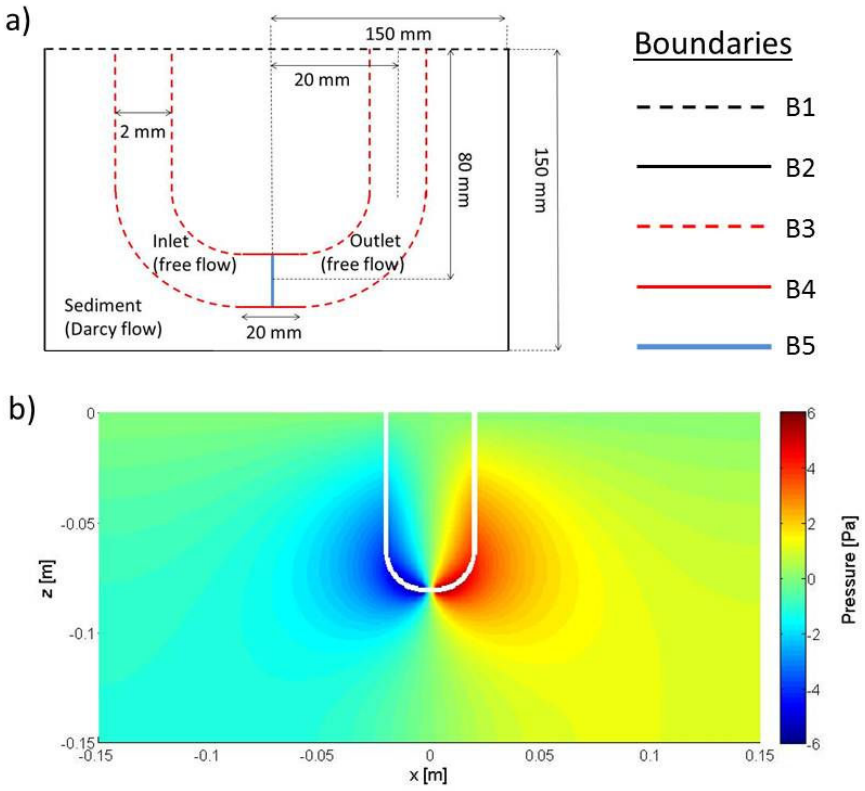

Figure 1: Geometry of the model area (a) and pressure field in the sediment surrounding the burrow resulting from the modeled pumping activity of the chironomid (b).

The solute transport of the inert tracer was calculated using the advection-diffusion equation,

$$\frac{\partial c}{\partial t} + \nabla \cdot \left(- \varepsilon D \nabla c \right) + \mathbf{u} \nabla c = 0 \qquad (3)$$

where D is the diffusion coefficient in water and ε the sediment porosity. We used a D value of 1.5 10^{-9} $m^2 s^{-1}$, which is close to the diffusivity of many substances in aqueous solution and a porosity ε of 0.8, which is typical for unconsolidated sediments. For simplicity we neglected any effects of sediment tortuosity in this conceptual numerical study.

In the presented model study we first calculated the steady state velocity field based on equations 1 and 2 and used the resulting field to calculate transient development of the inert tracer concentration.

Boundary	Free flow	Darcy flow	Solute transport
B1	$p = 0$	$p = 0$	$c = 1$
B2	-	no flow	no flux
B3	$\mathbf{u} = 0$	$p_{sed} = p_{tube}$	c = 1
B4	$\mathbf{u} = 0$	no flow	no flux
B5	laminar inflow/outflow	-	-

Table 1: Boundary conditions for the domain and subdomain boundaries as indicated in Figure 1a. p_{tube} is the hydraulic pressure in the tube, p_{sed} the pressure in the surrounding sediment. At boundary 5 there is a sink in the inlet domain and a source of the same strength in the outlet domain.

2.2 Boundary conditions

The boundary conditions for the various boundaries between the individual domains and subdomains are given in table 1. For the location of the individual boundaries see Figure 1a.

The pumping activity of the chironomid was mimicked by separating the tube into an inlet and an outlet subdomain using boundary 5 (Figure 1a). An outflow of 6.8 10^{-8} m^3 s^{-1} corresponding to an average flow velocity of 2 cm s^{-1}, which is close to the values reported in laboratory studies[1,2] was imposed at boundary 5 at the inlet side. The same flow was pressed into the outlet domain at boundary 5. Since very high pressure gradients occurred in the close vicinity of boundary 5, the tube walls 1 cm next to the boundary 5 (boundary 4) were modeled as completely impermeable walls to avoid high short circuit flow in the sediment.

The coupling between the burrow tube wall and the sediment starting 1 cm before and after boundary 5 was implemented by equalizing the pressure between tube and sediment. This means that the pressure exerted by the pumping chironomid is the driving force of the advective flow in the sediment. Fluid loss from the tube to the sediment by leaking through boundary 3 is negligible since the Darcy velocity is much smaller compared to the free flow. Therefore, the no slip condition ($\mathbf{u}$=0) was applied to at the tube wall (boundary 3).

3 RESULTS

3.1 Fluid Flow

In order to maintain the fluid flow against the viscous forces in our model domain, the chironomid has to exert a pumping pressure of 6 Pa in the center of the tube. The pressure field in the tube propagates into the sediment with decreasing pressure from the outlet branch to the inlet branch and decreasing pressure from the deepest point of the tube to the sediment surface (Figure 1b). This pressure field is the driving force for the Darcy flow in the sediment (Figure 2a). The highest absolute flow velocities in the sediment (1.4 10^{-8} m s^{-1} for κ=10^{-14} m^2 to 1.4 10^{-5}

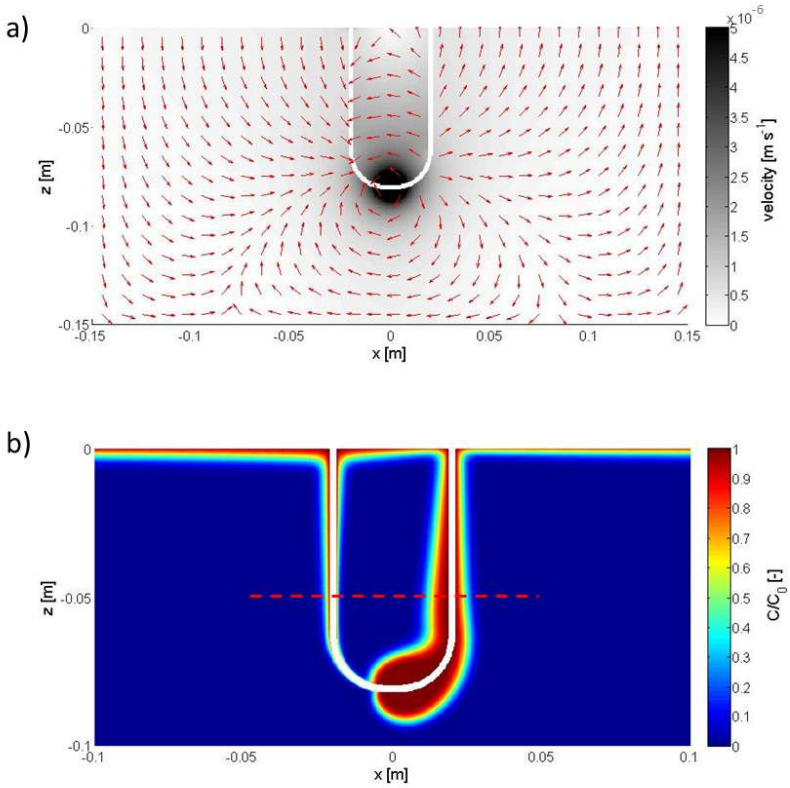

Figure 2: Flow velocity field (a) and normalized concentration distribution (ratio between sediment concentration C and concentration at the sediment surface C_0) of an inert tracer after 3600 s (b) calculated for a permeability of 10^{-11} m^2. The red line denotes the transect for the data shown in Figure 3.

m s^{-1} for κ=10^{-11} m^2) are observed close to the chironomid larva (deepest point of the tube). These values decrease nonlinearly with distance from this location (Figure 2a). Between the tubes, the pore water flow is mainly directed from the outlet branch towards the inlet branch, while water flows from the sediment-water interface (SWI, boundary 1) into the sediment in the vicinity of the inlet and out of the sediment across the SWI in the vicinity of the outlet.

3.2 Solute transport

The impact of the advective flow the solute transport in the sediment can be relevant. Figure 2b shows the distribution of the inert tracer after 3600 s for a permeability of κ=10^{-11} m^2. The distribution of the tracer is characterized by a high asymmetry between the inlet branch and the outlet branch of the tube. This asymmetry stems from the transport of water towards the tube at the inlet branch and the transport of water into the sediment at the outlet branch. The highest intrusion of the tracer is observed at the outlet branch close to the chironomid where the tracer

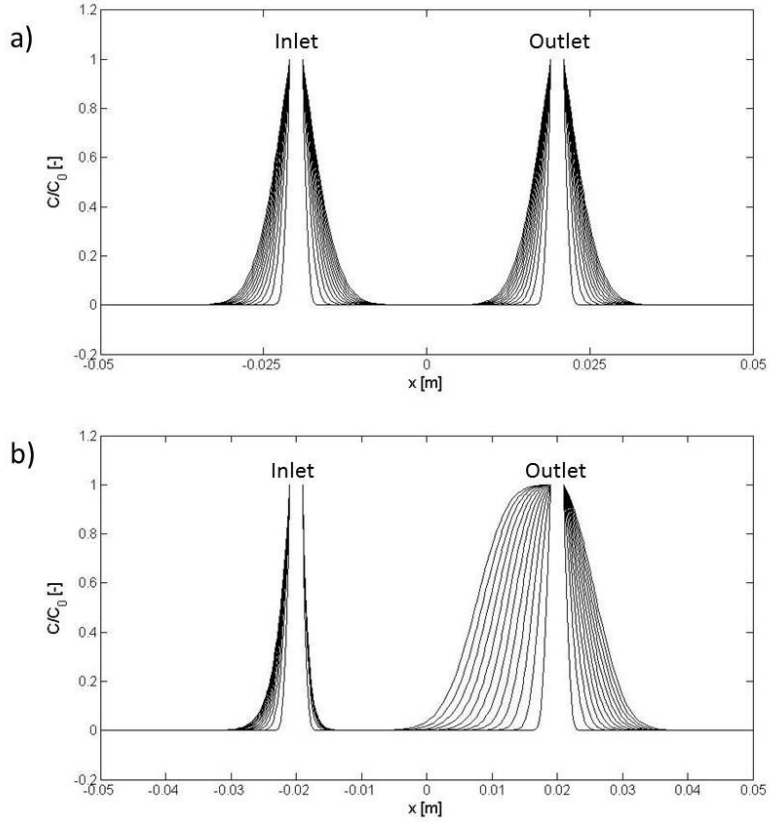

Figure 3: Development of inert tracer distribution from 200 to 6800 s in 600 s steps along the red line indicated in Figure 2b. a) Permeability 10^{-14} m^2 b) Permeability 10^{-11} m^2

intrudes up to 2 cm from the burrow wall into the sediment. The intrusion depth along the outlet branch decreases with increasing distance from the larva. In contrast, the intrusion depth of the tracer along the inlet branch increases with increasing distance from the larva (Figure 2b). Interestingly, the intrusion of tracer from the sediment-water interface into the sediment is higher in the zone around the inlet compared to the zone around the outlet. This is due to the negative pressure at the inlet, which results in a water flow into the sediment, while tracer-containing water is pressed into the water column in the vicinity of the outlet which counteracts the diffusive transport into the sediment. In both cases, this effect decreases with increasing distance from the tubes.

It is evident that the influence of the pressure induced advection in the sediment is highly dependent on the permeability of the sediment. Figure 3 compares the temporal development of the tracer distribution along a horizontal transect in 5 cm depth (indicated by the red line in Figure 2b). At a permeability of 10^{-14} m^2, the development of the tracer distribution is practically identical at inlet branch and outlet branch and diffusion is the dominant transport process (Figure 3 a). In contrast, for a permeability of 10^{-11} m^2, the development of the tracer distribution varies

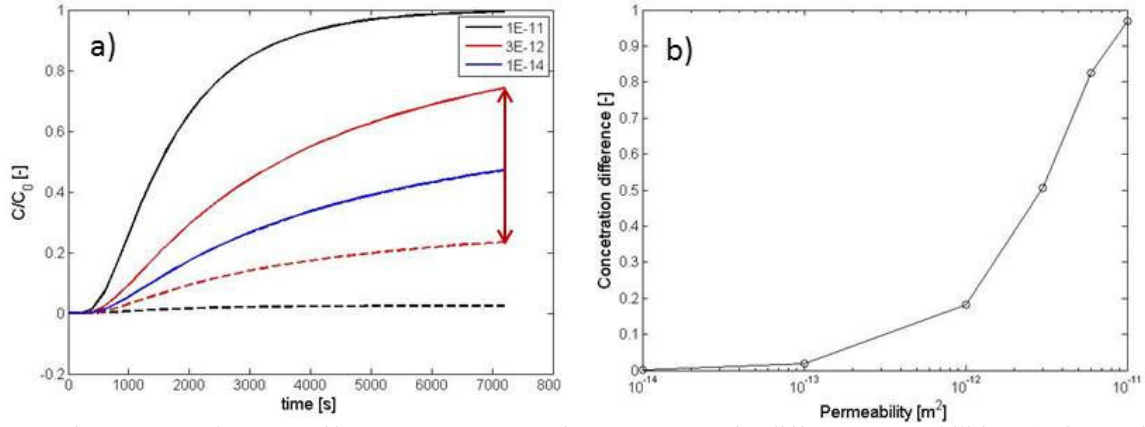

Figure 4: Development of inert tracer concentration over 7200 s for different permeabilities. a) Time series calculated for two point probes. The probes were located between inlet and outlet at 5 cm depth at 3 mm distance from the tube walls. Dashed lines indicate data recorded close to the inlet and solid lines data recorded close to the outlet. The dashed blue line cannot be seen because its course is identical with the solid blue line. b) Concentration difference between the probes described in a after 2700 s as indicated by the arrow in Figure 4a.

significantly between inlet and outlet branches. This discrepancy is mostly pronounced in the sediment region between the in- and outlet branches. While tracer is transported advectively in the sediment close to the outlet branch, the diffusive transport into the sediment from the inlet branch is suppressed by the advection of tracer-free pore water. The same effect is observed on the sides of in- and outlet branches facing the domain boundaries even though it is much less pronounced in these directions.

The dependence of bioirrigation induced pore water advection on the sediment permeability κ is analyzed in Figure 4. Figure 4a shows the breakthrough curves observed in 3 mm distance from the inlet and outlet branches (x=-0.016 m and 0.016 m) at 5 cm depth. While there is no evident difference between the concentrations close to the inlet and outlet branches for $\kappa=10^{-14}$ m^2. Almost no tracer was observed at the inlet branch for $\kappa=10^{-11}$ m^2. In contrast, the concentration 1 cm apart of the outlet branch was almost identical to the concentration at the boundary. The effect was not as strongly pronounced for $\kappa=3\ 10^{-12}$ m^2. The dependence of the tracer intrusion is highly non-linear (Figure 4b). The difference between the concentrations observed at the in- and outlet branches after 7200s is less than 3% for $\kappa<1\ 10^{-13}$ m^2, while the difference increases much stronger for higher permeabilities (Figure 4b).

3 DISCUSSION

The approach presented in the paper is a first step towards a more mechanistic understanding of bioirrigation in permeable freshwater sediments. Still, there is more work necessary to develop a comprehensive model which provides more quantitative results. In our study, we assumed a constant pumping activity instead of intermittent pumping as observed in nature. Since the pumping activity of *C. plumosus* covers over 50% of the time[2], a more complex model which considers transient pumping should provide similar qualititative, though less strongly

pronounced results for the solute transport. The same applies to the fact that we used a 2-D domain instead of a 3-D domain in order to save computation time. In a 3-D domain, we will expect a slightly lower tracer intrusion similar to the difference between 1-D and 1-D radially symmetric diffusion models. Still, our general conclusions are not affected by the simplifying use of a 2-D domain.

A potential further extension of our model is the consideration of reactive solute transport using simple degradation kinetics as well as later on complex reaction networks. This step will give a more detailed insight into the relevance of bioirrigation induced advection on nutrient turnover and redox cycling in aquatic sediments.

Our model study has shown that the pumping activity of macrofouna like *C. plumosus* in U-shaped, non-blindly ending tubes can indeed induce pore water advection in the surrounding sediments and therefore backs the laboratory obervations reported recently[3]. The importance of advection on the solute transport in the sediment shows a highly non-linear dependence on the sediment permeability. The values used in this conceptual study cover a wide range which is also observed in the field. Therefore, the potential occurrence of bioinduced porewater advection needs to be addressed on a case to case basis. Further studies, which combine laboratory experiments like the PET tracer study[3] with numerical modeling as outlined in this manuscript are necessary to extend the understanding of the role of tube dwelling macrofauna in sediment biogeochemistry. Still, it is important to keep in mind that the assumption of diffusion dominated transport in bioirrigated sediments may not always hold. This assumption is, for example, the basis of the radially symmetric tube models which are widely used to describe solute dynamics in bioirrigated sediments[6].

REFERENCES

[1] M. R. Morad, A. Khalili, A. Roskosch and J. Lewandowski, "Quantification of pumping rate of Chironomus plumosus larvae in natural burrows", *Aquatic Ecology* **44** (1): 143-153 (2010).

[2] A. Roskosch, M. Hupfer, G. Nutzmann and J Lewandowski, "Measurement techniques for quantification of pumping activity of invertebrates in small burrows", *Fundamental and applied Limnology* **178**(2): 89-110 (2011).

[3] A. Roskosch, J. Lewandowski, R. Bergmann, F. Wilke, W. Brenner and R. Buchert, "Identification of transport processes in bioirrigated muddy sediments by [18F]fluoride PET (Positron Emission Tomography)", *Applied Radiation and Isotopes* **68** (6): 1094-1097 (2010).

[4] F. Meysman, E. S. Galaktionov and J. J. Middelburg, "Irrigation patterns in permeable sediments induced by burrow ventilation: a case study of Arenicola marina", *Marine Ecology-Progress Series* **303**: 195-212 (2005).

[5] J. Bear, *Dynamics of Fluids in Porous Media*, Dover, (1972).

[6] R. C. Aller, "Quantifying Solute Distributions in the Bioturbated zone of Marine-Sediments by defining an average Microenvironment", *Geochimica et Cosmochimica Acta* **44** (12): 1955-1965, (1980).